ELSEVIER

Biochimica et Biophysica Acta 1285 (1996) 146–154

BIOCHIMICA ET BIOPHYSICA ACTA
BBA

Utilization of monensin for detection of microdomains in cholesterol containing membrane

S. Bransburg-Zabary, E. Nachliel, M. Gutman *

Laser Laboratory for Fast Reactions in Biology, Department of Biochemistry, George S. Wise Faculty of Life Sciences, Tel Aviv University, Ramat Aviv 69978, Israel

Received 15 May 1996; revised 19 July 1996; accepted 19 July 1996

Abstract

The effect of cholesterol on the monensin mediated proton–cation exchange reaction was measured in the time-resolved domain. The experimental system consisted of a black lipid membrane equilibrated with monensin (Nachliel, E., Finkelstein, Y. and Gutman, M. (1996) Biochim. Biophys. Acta 1285, 131–145). The membrane separated two compartments containing electrolyte solutions and pyranine (8-hydroxypyrene 1,3,6-trisulfonate) was added on to one side of the membrane. A short laser pulse was used to cause a brief transient acidification of the pyranine-containing solution and the resulting electric signal, derived from proton–cation exchange, was measured in the microsecond time domain. Incorporation of cholesterol had a clear effect on the electric transients as measured with Na^+ or K^+ as transportable cations. The measured transients were subjected to rigorous analysis based on numeric integration of coupled, non-linear, differential rate equations which correspond with the perturbed multi-equilibria state between all reactants present in the system. The various kinetic parameters of the reaction and their dependence on the cholesterol content had been determined. On the basis of these observations we can draw the following conclusions: (1) Cholesterol perturbed the homogeneity of the membrane and microdomains were formed, having a composition that differed from the average value. The ionophore was found in domains which were practically depleted of phosphatidylserine. (2) The diffusivity of the protonated monensin (MoH) was not affected by the presence of cholesterol, indicating that the viscosity of the central layer of the membrane was unaltered. (3) The diffusivity of the monensin metal complexes (MoNa and MoK) was significantly increased upon addition of cholesterol. As the viscosity along the cross membranal diffusion route is unchanged, the enhanced motion of the MoNa and MoK is attributed to variations of the electrostatic potential within the domains.

Keywords: Monensin; Cholesterol; Microdomain; Time-resolved polarization; Polarization

1. Introduction

In the preceding publication [1] we described an experimental method, based on asymmetric pulse acidification of a bilayer membrane, that can quantitate the physical properties which control the flux of uncharged hydrophobic bodies across the membrane.

Abbreviations: PC, phosphatidylcholine; PS, phosphatidylserine; ch, cholesterol; MoM, monensin-metal complex; MoH, protonated monensin; ϕOH, ϕO^-, 8-hydroxypyrene in its protonated and ionized state, respectively.

* Corresponding author. Fax: +972 3 6415053.

PII S0005-2736(96)00148-4

That study clearly discriminated between the effects of viscose drag and the dipolar field as independent modulators of the diffusion across the membrane. Encouraged by the results we employed this method to investigate the effect of cholesterol on the rigidity of the membrane and the intensity of the electrostatic potentials. According to the common knowledge that cholesterol increases the rigidity of the membrane [2–4] we were expecting to measure a slower diffusion of the MoH in cholesterol-enriched membranes. Cholesterol also affects the intensity of the membrane's dipolar field. The dipolar field of phospholipid membranes is generated by the ordered dipoles of the fatty acid's carbonyls and the ordered water at the interface [5–7]. Cholesterol, when incorporated into bilayers [8] or monolayers [9] is oriented normal to the surface with its dipole pointing in the same direction as that of the carbonyls or the ordered water. As a result the measured field was increased upon incorporation of cholesterol to a membrane. Based on this information it was expected that addition of cholesterol will retard the diffusion of the polarized MoNa and MoK complexes even more than that of the nonpolar MoH. Our experimental measurements demonstrated that both expectations were not fulfilled. The diffusivity of MoH, as measured across the membrane's acyl chain region, was not reduced in cholesterol-containing membrane, indicating that the viscosity along the cross-membranal trajectory of the diffusing monensin is hardly affected by the incorporated cholesterol. In parallel we found that the presence of cholesterol increased the cross-membranal diffusivity of the dipolar MoNa and MoK complexes. This finding implies that in the immediate vicinity of the monensin the local dipolar field is not equal to the average one as measured by more macroscopic techniques [7,8].

The detailed analysis of the experimental tracing yielded, among other parameters, the number of phosphatidylserine molecules which are at proton transfer range from the monensin-metal complex. The results indicate that addition of cholesterol caused a sharp fall in that number. In the absence of cholesterol, there are about 25 phosphatidylserine (PS) carboxylates per MoM molecule. In the presence of cholesterol we measured less than one. This observation indicates that the homogeneity of the membrane was lost and microdomains, poor in PS and rich in PC and cholesterol, are formed. These microdomains appear to be a better solvent for the monensin metal complexes.

The effect of cholesterol on the domains structure in phospholipid membrane has been measured at temperatures close to the transition temperature where both the liquid-crystal and the gel states coexist [9–11]. It was found that, under these conditions, cholesterol breaks down the domain and enhances the homogeneity of the membrane. In the present communication we report that cholesterol can also impose domain formation in the liquid-crystal state of the membrane. The energetic considerations which account for this behavior are discussed.

2. Materials and methods

The observation cell, the preparation of membrane and the equilibration with monensin were carried out exactly as in our previous publication [1].

The excitation of the dye was attained by an LCI nitrogen laser delivering to the observation cell a 1 ns pulse of ≈ 100 μJ ($\lambda_{max} = 347$ nm). Because of the lower energy, in comparison with the conditions used in our previous publication, the concentration of pyranine in the cell was raised up to 900 μM. The measuring circuit used for monitoring the transient was essentially that described before [1], except that a 60 dB voltage amplifier (Analog Modules 324-A-4-B) substituted the current/voltage converter and the conducting electrolyte concentration (choline chloride) was increased to 1 M.

The phospholipids (Avanti, egg phosphatidylcholine and brain phosphatidylserine, at 3:2 w/w ratio) were mixed with cholesterol (all in $CHCl_3$) to the desired proportions (w/w), dried up by evacuation and dissolved either in hexane or in decane to final concentrations of 0.5% and 1.5% (w/v), respectively.

For each cholesterol/phospholipid mixture, a new bilayer was made up and equilibrated for 20 min with monensin (20 μM, added on both sides). At the end of the equilibration 900 μM pyranine was added to the driving (D) side of the cell and the pulsing by the laser was commenced. The electric signals were measured in the presence of saturating concentrations of NaCl (150 mM and up) or KCl (250 mM and up).

For each membrane the transients were measured with increasing salt concentrations to verify that the dynamics and shape of the signal are independent of the salt concentration.

The numeric analysis of the transient was similar to that described previously [1].

3. Results

3.1. The polarisation transient driven by the proton pulse

A typical voltage transient generated by pulse acidification of the membrane is shown in Fig. 1. The experiment, carried out with a cholesterol-free membrane, bears all the characteristic features discussed in the preceding paper [1]. The most initial phase of the transient is a fast unresolved positive spike. It is followed by a brief, negative transient which evolves into a long positive wave that contains most of the data points.

Experiments that were carried out in the presence of cholesterol were very similar in shape and no extra features were observed (Fig. 2). Each sample was subjected to irradiation at two levels of pulse energy, yielding signals with amplitudes of ≈ 12 μV and ≈ 2 μV, respectively. (Please note that in the present communication the transients are of voltage, not current, thus the shape of the curves is not the same).

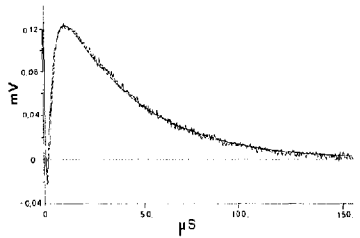

Fig. 1. Polarization transient of a black lipid membrane impregnated with monensin subjected to pulse acidification of one side. The membrane, made as in Section 2, was equilibrated for 20 min with 20 μM monensin in a solution containing 1 M choline chloride, 150 mM NaCl, (900 μM pyranine was added on the D side (see Ref. [1] for more details). The membrane was irradiated by 256 laser pulses (= 100 μJ 334.7 nm) at a repetition rate of 0.2 Hz. The electric potential built between the two sides of the membrane was measured by a fast responding voltage amplifier and the signals were averaged before display. The solid line superpositioned over the experimental signals is the reconstructed dynamics generated by the procedure detailed in Ref. [1].

3.2. Numeric analysis of the observed transients

The numeric reconstruction of the signals followed the same procedure and program as described before [1]. Each signal was analyzed de novo and the adjustable parameters were varied until the calculated charge disbalance transient (ΔQ vs. t) matched the measured one ($\Delta V/C$ vs. t), where ΔV is the measured voltage and C is the capacitance of the membrane. The fitting ignored the poorly resolved early spikes and concentrated on the main positive voltage wave.

Black lipid membrane preparations are quite notorious for their instabilities. If technically possible, it is better to carry out a full set of measurements on the same membrane. In the present study this was beyond reach as cholesterol cannot be incorporated into a pre-existing membrane.

To compensate for this handicap and increase confidence in the analysis, we repeated the kinetic measurements, as carried out for each lipid/cholesterol ratio, 2 to 4 times. Each membrane was made on another day and the kinetics were measured both at the high and the low outputs of the exciting laser pulse. The amplitudes of the measured signals, recorded at high and low laser intensity, vary by 5–6-fold (see Fig. 2). Yet, in spite of these variations, the numeric reconstruction of the signals converged into the same set of rate constants. The only parameter that varied in proportion with the amplitude was the size of the perturbation.

The fitted curves, shown in Figs. 1 and 2, document the results of experiments carried out with different cholesterol content using either Na^+ or K^+ as transportable cations both at high and low intensities of the laser pulse.

The numeric reconstruction was carried out for all the experimental signals as measured with membranes where the cholesterol content varied from zero to 30%. The quality of the fits was as exemplified in

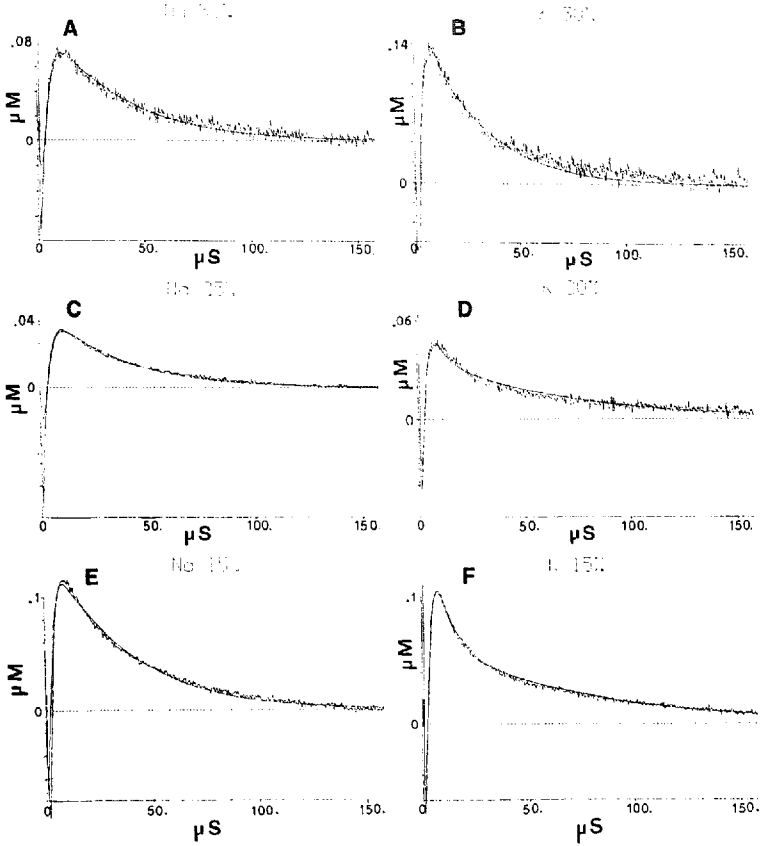

Fig. 2. The effect of cholesterol on the polarization transients measured with phospholipid membranes equilibrated with monensin. The experiments were measured as described in Fig. 1 except that cholesterol was added to the lipid mixture at the concentration marked in each frame. The transportable cations were Na^+ (Frames A, C, E) or K^+ (Frames B, D, F). The laser intensity in C and D was lowered to ≈ 20 μJ/pulse. The smooth curves are the numeric reconstruction of the dynamics.

Table 1
The kinetic and equilibrium constants characterizing H^+/Na^+ exchange by monensin in the presence of varying cholesterol content

% Chol.		0%	1%	5%	10%	15%	20%	25%	30%
PS (μM)		630	300	15.0	44.0	66.0	45.0	48.0	39.0
PS/MoM		22.0	0.85	0.75	0.75	0.75	0.75	0.75	0.75
k_3; 10^9 $M^{-1}s^{-1}$	$MoNa + H^+$	7.5	10.5	10.5	10.5	10.5	10.5	10.5	10.5
k_6; 10^8 $M^{-1}s^{-1}$	$MoH + Na^+$	3.0	3.0	3.0	3.0	3.0	3.0	3.0	3.0
k_7; 10^{10} $M^{-1}s^{-1}$	$Mo^- + H^+$	0.5	0.5	0.5	1.0	1.0	1.0	1.0	1.0
k_9; 10^4 $M^{-1}s^{-1}$	$Mo^- + Na^+$	2.0	2.0	2.0	2.0	2.0	2.0	2.0	2.0
k_{20}; 10^5 s^{-1}	$MoH_D \rightarrow MoH_R$	6.7	5.8	5.8	5.7	6.0	6.2	6.4	6.2
k_{22}; 10^5 s^{-1}	$MoNa_D \rightarrow MoNa_R$	0.4	0.4	0.4	0.4	0.45	0.85	1.7	6.0
k_{31}; 10^9 $M^{-1}s^{-1}$	$MoH + \Phi O^-$	1.2	1.2	1.2	1.2	1.2	1.2	1.2	1.2
k_{33}; 10^{10} $M^{-1}s^{-1}$	$PSH + \Phi O^-$	1.0	1.0	1.0	0.8	0.8	0.8	0.8	0.8
pK (H^+)	MoNaH	4.8	5.25	5.7	6.22	6.22	6.28	6.3	6.3
pK (Na^+)	MoNaH	1.0	1.46	1.96	2.55	2.85	3.0	3.3	3.4
pK	MoH	6.62	6.62	6.62	6.62	6.38	6.35	6.1	6.1
pK	MoNa	2.82	2.83	2.88	2.95	3.01	3.07	3.125	3.2

The parameters listed in each column represent the measurements carried out at the given cholesterol value. The units of the parameters are given in the first column.

Fig. 2 and the rate constants are listed in Table 1 (for Na^+) and Table 2 (for K^+).

3.3. Visualization of the effect of cholesterol on the polarization transient

Due to daily variations in the experimental conditions, direct comparison between experiments carried out with different cholesterol contents is inappropriate.

To demonstrate the effect of the cholesterol content on the shape and magnitude of the electric signal, we chose to reconstruct the experiments at the idealized virtual reality of the computation space, where the initial reactant concentrations could be equalized and the parameters, given in Table 1 or Table 2, were

Table 2
The kinetic and equilibrium constants characterizing H^+/K^+ exchange by monensin in the presence of varying cholesterol content

% Chol.		0%	1%	5%	10%	15%	20%	25%	30%
PS (μM)		670	14.0	26.0	37.0	49.0	52.0	56.0	72.0
PS/MoM		20.0	0.85	0.75	0.75	0.75	0.75	0.75	0.75
k_3; 10^{10} $M^{-1}s^{-1}$	$MoK + H^+$	0.7	0.7	0.7	0.7	0.7	0.7	1.0	1.0
k_6; 10^9 $M^{-1}s^{-1}$	$MoH + K^+$	2.4	2.4	2.4	2.4	2.4	2.4	2.4	2.4
k_7; 10^{10} $M^{-1}s^{-1}$	$Mo^- + H^+$	0.7	0.7	0.7	0.7	0.7	0.7	0.5	0.5
k_9; 10^4 $M^{-1}s^{-1}$	$Mo^- + K^+$	2.0	2.0	2.0	2.0	2.0	2.0	2.0	2.0
k_{20}; 10^5 s^{-1}	$MoH_D \rightarrow MoH_R$	6.7	6.8	6.8	6.2	6.0	6.0	6.7	6.5
k_{22}; 10^5 s^{-1}	$MoK_D \rightarrow MoK_R$	11.5	18.0	18.0	40.0	27.0	40.0	56.0	65.0
k_{31}; 10^9 $M^{-1}s^{-1}$	$MoH + \Phi O^-$	1.2	1.2	1.2	1.2	1.2	1.2	1.2	1.2
k_{33}; 10^{10} $M^{-1}s^{-1}$	$PSH + \Phi O^-$	1.8	0.8	0.7	0.8	0.6	0.6	0.6	0.6
pK (H^+)	MoKH	4.95	5.16	5.52	6.0	6.0	6.0	6.0	6.0
pK (K^+)	MoKH	0.15	0.38	0.9	1.4	1.72	1.84	2.22	2.32
pK	MoH	6.62	6.62	6.62	6.62	6.4	6.38	6.1	6.1
pK	MoK	1.82	1.84	1.92	2.02	2.12	2.22	2.32	3.42

The parameters listed in each column represent the measurements carried out at the given cholesterol value. The units of the parameters are given in the first column.

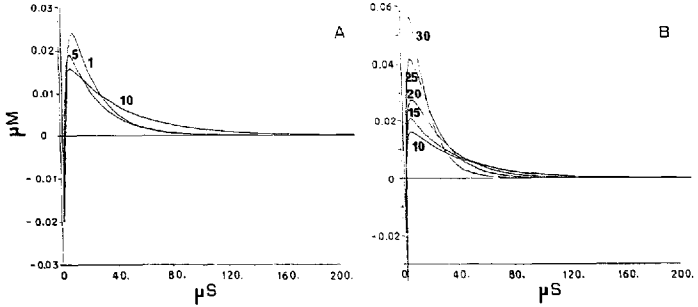

Fig. 3. Simulation of the polarization transients under equal boundary conditions. The curves are the numeric reconstruction of the dynamics with 1%, 5% and 10% cholesterol (Frame A) or 10%, 15%, 20%, 25% and 30% cholesterol in Frame B. All other concentrations (monensin, perturbation pulse, pyranine, Na^+ and initial pH) were set to be equal. The rate constants and PS/MoM ratio used for the reconstruction were taken from Table 1.

used to reproduce the dynamics for the various cholesterol contents of the membranes.

As shown in Fig. 3, the effects of cholesterol on the polarization signal vary with its intramembranal content. Below 10% it suppressed the transient and stretched the perturbation over time (Fig. 3A). At higher concentrations, the trend is reversed (Fig. 3B); the amplitude increases while the relaxation time becomes shorter.

A similar pattern was obtained with K^+ as a transportable cation (not shown).

4. Discussion

The simulated transients representing the signals as shown in Fig. 3 (A and B) demonstrate the complexity of the cholesterol effect. At low content it suppresses the electric signal while at higher content the transient increases both in magnitude and rate. Any attempt to quantitate the observed effect of cholesterol just by referring to amplitudes and time constants will not serve to clarify why cholesterol causes these effects. As argued in the preceding publication, the understanding of the dependence of the observed signal on the cholesterol content must rely on the molecular parameters listed in Tables 1 and 2. In the following discussion we shall implement this approach.

4.1. Quantitative evaluation of the rate constants

The chemical events which drive the electric transient are initiated by protonation of the carboxylate of the phosphatidylserine moieties (see Scheme 2 in the preceding publication [1]). The rate constant of this reaction (k_{11} in Tables 1 and 2) has a magnitude typical of a diffusion controlled reaction and the rate is independent of the cholesterol content. In parallel, the diffusion controlled reaction between ϕO^- and the protonated phosphoserine headgroup is also unaffected by cholesterol. Thus it can be concluded that incorporation of cholesterol does not modify the accessibility of the phosphoserine moieties to the bulk [12]. The same conclusion is reached with respect to the accessibility of the monensin-metal carboxylate. The rates of its protonation by H^+ or deprotonation by ϕO^- (k_7 and k_{31} in Tables 1 and 2) are diffusion-controlled according to their magnitude and are not affected by the incorporation of cholesterol.

While the rates of interaction between monensin and water-soluble ions seem to be unaffected by cholesterol, some equilibrium constants like the dissociation of MoH (pK_{78}) and the dissociation reac-

tions of the ternary complex (pK_{43} and pK_{65}) exhibit a clear dependence on the cholesterol content. We consider these changes as evidence that the immediate environment surrounding the monensin changes upon addition of cholesterol yet a mechanistic interpretation of the measured effect is still premature.

4.2. The rate of transmembranal diffusion

As detailed in the preceding publication [1], both MoH and MoM diffuse across the membrane as uncharged complexes. The MoH complex, devoid of dipole moment, is retarded only by a viscous drag while the MoM complex, due to its dipole moment, has also to overcome the energy barrier set by the dipolar field of the membrane. A quantitative evaluation of the effect of cholesterol on the diffusivity of the two complexes can discriminate between the variation in viscosity and modulation of the electrostatic potential in the immediate vicinity of the diffusing complex.

The dependence of the rate of cross-membranal diffusion of MoH and MoM are shown in Fig. 4. It is evident that cholesterol does not increase the viscous drag. The rate constant of MoH diffusion across the membrane is constant and equal to that measured in the absence of cholesterol. The drag, as calculated for the cross-membranal diffusion of monensin, is compatible with local viscosity of ≈ 1 poise. There are numerous experiments based on a variety of methodologies (fluorescence polarization [2], NMR [3] and photoaccoustic measurements [4]) which consistently record an incremental viscosity of the membrane upon addition of cholesterol. In all these experiments the gaugement of the viscosity was along the membrane's surface. In the present study it is measured normal to the plane. Thus our measurements are not in contradiction to common knowledge but illuminate an aspect as yet untouched.

The cholesterol molecules in the membrane are arranged with their 3-OH moiety exposed to the water, while their rigid hydrophobic body inserted between the acyl chains [11,13–15]. In this position they function as a spacer between the polar headgroups, but do not interact with them [13,16]. The insertion of the cholesterol into the membrane rigidifies the outer section of the acyl chains, while at the inner section of the low dielectric matrix the disorder is increased [17]. The unaltered rate of MoH diffusion, from one side of the membrane to the other, implies that the initial equilibrium placement of the carrier within the membrane is such that its cross

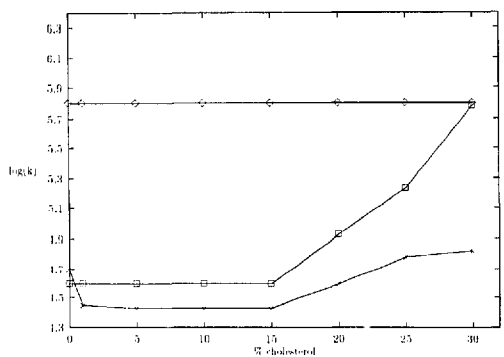

Fig. 4. The effect of cholesterol content on the rate of monensin diffusion across the membrane. ◇, The rate constant of MoH diffusion. □, The rate constant of MoNa diffusion. ×, The rate constant of MoK diffusion.

membranal diffusion mostly transverses the midsection of the membrane where the rigidifying effect of cholesterol is not expressed.

These conclusions are in accord with the theoretical calculations of the free energy of monensin transfer from water to membrane. The monensin molecule is mostly hydrophobic and only its carboxylate region carries some local charges. As a result, upon dissolving in the membrane, most of the ionophore will be submerged in the low dielectric matrix of the membrane while only the carboxylate region is exposed to the aqueous phase. Upon diffusion across the membrane the ionophore's center of mass transverses only the midsection of the membrane. In parallel the ionophore rotates so that its hydrophilic segment faces the nearest lipid-water boundary (Ben-Tal and Gutman, unpublished results).

The diffusion of the MoM complexes is controlled both by the viscous drag and the interaction between the molecular dipole and the dipolar field of the membrane [1]. The enhanced diffusivity of both MoNa and MoK across the membrane (see Fig. 4) as a function of the cholesterol content implies a diminished electrostatic barrier in the vicinity of the monensin. This conclusion contradicts the observations of Franklin and Cafiso [7] or Simon et al. [8] that cholesterol increases the dipolar field of the membrane. This apparent discrepancy might be explained by assuming that the environment sampled by our gauge particle differs greatly from the averaged value of the membrane. The incorporation of cholesterol appears to break the homogeneity of the membrane and microdomains of different lipid composition are formed. These cholesterol-rich PC domains are the favored site for the binding of the ionophore. Due to the short decay length of the dipolar field [6], the local intensity within the domain may differ from that measured by less resolving methods [7,8].

4.3. Proton exchange between surface groups

The mechanism of proton transfer between immobile surface groups has been reviewed recently by Gutman and Nachliel [12]. A proton released by one site can be taken up by the adjacent one with a varying probability of escape to the bulk. Sites that are close enough for their Coulomb cages to overlap will exchange proton with marginal loss to the bulk. As the distance between the sites increases, the efficiency of proton transfer between them falls sharply and most of the protons will be lost to the bulk. Time-resolved kinetics measurements have shown that for reactants placed at a distance comparable to the Coulomb cage radius, the apparent rate constant for proton transfer has a magnitude of approx. $1-3 \cdot 10^{10}$ [12].

The proton pulse causes a transient protonation of the whole surface of the membrane. Yet the measured electric signal is generated only by those protons which react with PS molecules that are located within a proton transfer range ($\approx 20-30$ Å) from a monensin molecule. Analysis of the experimental curves, measured in the absence of cholesterol, indicated that the rate of proton transfer from protonated PS to MoNa has a rate constant of $\approx 1 \cdot 10^{10}$ and about 25 molecules of PS are available for each monensin molecule to serve as a proton donor. Assuming a random distribution of phospholipid in the membrane and a surface area of $\approx 50-60$ Å^2 per phospholipid headgroup, then at a relative abundance of 40% PS, this number of PS molecules will be found in a domain having a width of about 30 Å surrounding each MoM complex. Each PS molecule within this boundary, if protonated, has an appreciable probability to transfer its proton to the monensin's carboxylate before the proton is lost to the bulk. Upon addition of cholesterol the number of PS molecules located at a proton transfer distance from the monensin drops sharply to less than one, indicating that the immediate perimeter of the monensin (i.e. ≈ 30 Å wide ring) is effectively depleted of phosphatidylserine.

4.4. The effect of cholesterol on the microscopic structure of the membrane

The thermodynamic favored position of cholesterol in the membrane is along the extended acyl chains [13–17] with no interactions with the headgroups. Due to the fact that cholesterol is only a spacer between the headgroups, its insertion between phospholipids differing in the intensity of their headgroups' interaction will affect the overall energetics of the system. Headgroups which interact poorly with each other, like phosphatidylcholine, will have a higher affinity for cholesterol than PS or PE, which

have a stronger adherence between their polar headgroups [15–18]. Indeed the miscibility of cholesterol in PC is higher than in negatively charged phospholipids [18–20].

The incorporation of cholesterol in the lipid mixture had a dramatic effect on the efficiency of proton transfer between PS and monensin. The abundance of PS within the perimeter of MoM was diminished, indicating that its lipid composition differed from the average. The observed diminution of the proton transfer efficiency from protonated PS to MoM complex can be explained by two models. The first one is based on the observation of Spooner and Small [21] that triolein, added to a lipid bilayer, sinks deeper in a cholesterol-containing membrane. Such an explanation for our observation is inadequate as the measured accessibility of MoH to ϕO^- is not affected by addition of cholesterol (k_{31}, Tables 1 and 2). The alternative explanation is to assume that the monensin favors the PC, cholesterol-rich domains where the abundance of phosphatidylserine is low.

At a temperature close to the main transition temperature of a lipid membrane, addition of cholesterol upset the coexistence of the gel and liquid-crystal domains [21–24], shifting the system to a state of homogeneity. The domains reported in this study differ not in the ordering and interaction of their acyl chains but in the composition of the headgroup region. When the acyl chains are fully miscible, and the membrane is high above the transition temperature, the selective interactions between the polar headgroup impose unequal miscibility of the cholesterol [17–20] and phase separation in the liquid state of the membrane takes place.

Bloom and Thewalt [15] had pointed out that local properties must be monitored by the methodologies whose spectral time matches the propagation of the perturbation within the local domain. As shown in this study, we have employed the proton as a gauge molecule. By monitoring the rate of its reaction with the various membranal components we could discriminate the heterogeneity near the ionophore embedded in the multicomponent membrane.

References

[1] Nachliel, E., Finkelstein, Y. and Gutman, N. (1996) Biochim. Biophys. Acta 1285, 131–145.
[2] Saito, H., Araiso, T., Shrahama, H. and Fayama, T. (1991) J. Biochem. 109, 559–565.
[3] Weizs, K., Grobner, G., Stohrer, J. and Kothe, G. (1992) Biochemistry 31, 1100–1112.
[4] El-Sayed, M.Y., Guion, T.A. and Foyer, M.D. (1986) Biochemistry 25, 4825–4832.
[5] Gawrisch, K., Ruston, D., Zimmerberg, J., Parsegian, V.A., Rand, P.R. and Fuller, N. (1992) Biophys. J. 61, 1213–1223.
[6] Zheng, C. and Vanderkooi, G. (1992) Biophys. J. 63, 935–941.
[7] Franklin, J.C. and Cafiso, D.S. (1993) Biophys. J. 65, 289–299.
[8] Simon, S.A., McIntosh, T.J., Magid, D.A. and Needham, D. (1992) Biophys. J. 786–799.
[9] Silvius, J.R. (1992) Biochemistry 31, 3398–3408.
[10] Mouritsen, O.G. and Jargerson, R. (1994) Chem.Phys. Lip. 73, 2–25.
[11] Spink, C.H., Manley, S. and Breed, M. (1996) Biochim. Biophys. Acta 1279, 190–196.
[12] Gutman, E. and Nachliel, E. (1995) Biochim. Biophys. Acta 1231, 123–138.
[13] Stockton, G.W. and Smith, I.C.P. (1976) Chem. Phys. Lip. 17, 251–263.
[14] Yin, J.-J., Feix, J.B. and Hyde, J.S. (1987) Biophys. J. 52, 1031–1038.
[15] Bloom, M. and Thewalt, J.L. (1995) Mol. Membr. Biol. 12, 9–13.
[16] Corvera, E., Mouritsen, O.G., Singer, M.A. and Zuckermann, M.J. (1992) Biochim. Biophys. Acta 1107, 261–270.
[17] Shin, K.-H., Moieda, H., Fujiwara, T. and Akutsu, H. (1995) Biochim. Biophys. Acta 1238, 42–48.
[18] Brumfeld, V., Bach, D. and Miller, I.R. (1991) Eur. Biophys. J. 19, 287–293.
[19] Borochov, N., Wachtel, E.J. and Bach, D. (1995) Chem. Phys. Lipids 76, 85–92.
[20] Slater, S.J., Ho, C., Todder, F.J., Kelly, M.B. and Stubbs, C.D. (1993) Biochemistry 32, 3714–3721.
[21] Spooner, P.J.R. and Small, D.M. (1987) Biochemistry 26, 5820–5825.
[22] Slotte, J.P. (1995) Biochim. Biophys. Acta 1238, 118–126.
[23] Fiorini, R.M., Valentino, M., Glaser, M., Graton, E. and Curatola, G. (1989) Biochim. Biophys. Acta 939, 485–492.
[24] Spink, C.H., Maley, S. and Breed, M. (1996) Biochim. Biophys. Acta 1279, 190–196.